Three-dimensional display technologies in wave and ray optics: a review
(Invited Paper)

Hao Zhang (张 浩)*, Yan Zhao (赵 燕), Liangcai Cao (曹良才), and Guofan Jin (金国藩)

State Key Laboratory of Precision Measurement Technology and Instruments, Department of Precision Instrument, Tsinghua University, Beijing 100084, China

**Corresponding author: zhanghaocgh@hotmail.com*

Received February 13, 2014; accepted March 10, 2014; posted online May 20, 2014

Multiple three-dimensional (3D) display technologies are reviewed. The display mechanisms discussed in this paper are classified into two categories: holographic display in wave optics and light field display in ray optics, which present the 3D optical wave field in two different ways. Key technical characteristics of the optical systems and the depth cues of human visual system are analyzed. It is to be expected that these 3D display technologies will achieve practical applications with the increase of the optical system bandwidth.

OCIS codes: 120.2040, 100.6890, 090.2870.
doi: 10.3788/COL201412.060002.

1. Introduction

Display technology is the tool we use to transfer and present the visual information, and most of current display systems are two-dimensional (2D) ones. However, human visual system is more suitable in viewing three-dimensional (3D) scenes, because our surroundings are 3D. 3D display is superior compared to the conventional 2D display since it has the potential to accurately render sensations of depth, locations, and spatial relationships of the 3D scenes. Hence the development of 3D display technologies would hugely benefit the visualization of multidimensional data, such as medical imaging, virtual reality, and the entertainment industry.

Human visual system uses many depth cues to perceive the 3D information. These depth cues can be divided into two categories: physiological and psychological ones. Physiological cues are information related to a physical reaction of human eyes when viewing a 3D image and can provide us with accurate 3D information, which include accommodation, convergence, binocular disparity, motion parallax, and occlusion. In contrast, psychological cues are associated with our experiences on the visual information. The psychological effects include linear perspective, shading, color difference, shadow, texture, and other natural phenomena combined with memorized data in our brains. Human visual system uses all of these depth cues to determine relative depths in a 3D scene. In general, the better viewing experience can be achieved with more depth cues. The objective of 3D display is to reproduce the 3D images with the help of various depth cues.

3D display has a long history. The production of stereoscopic photographs began in early 19th century, starting with Sir Charles Wheatstone's stereoscope[1]. It directs two parallax views into the viewer's left and right eyes simultaneously to produce binocular disparity depth cue. Since then, prisms, color filter, polarization, and shutter based methods of stereoscopic system were invented[2−5]. Stereoscopic display systems utilize only binocular disparity to interpret the depth information of the 3D scenes, hence these kinds of systems would lead to mismatch between convergence and accommodation distances. Moreover, most users prefer 3D technologies that do not require them to use viewing aids, this has given rise to the class of autostereoscopic displays. Autostereoscopic systems separate the viewing zone with the help of spatial multiplexing methods, which present 3D information to the viewers without the need for special glasses. Examples of autostereoscopic display technologies include parallax based, volumetric, holographic, and light field displays. Parallax based techniques can be categorized into parallax barriers and integral photography. Ives[6] and Lippmann[7] provided these two early examples of spatial multiplexing techniques one century ago. Though invented much earlier, these two techniques can be seen as the subclasses of light field display, since they can achieve angularly control of the projected light field. In order to obtain autostereoscopic visual effect, light field displays use technologies that map each sample to the appropriate ray in free space, which can be descripted in ray optics. Recently, more advanced light field display techniques has been invented, including using anisotropic screens and layered 3D techniques. These techniques can reach better approximations of the real 3D light field[8,9]. Different with ray optics, holography uses wave optics to reconstruct the 3D scenes. It regards 3D light field as a complex optical wave field. Holography is an attractive way for displaying 3D images because it can reconstruct the whole optical wave field of the 3D scene and has the potential to provide all the depth cues that human eyes can perceive[10]. It enables steering light in a way that reconstructs the directions of light rays coming from 3D scene. The basic concept of holographic 3D display is "window view upon reality", and it can provide us with continuous parallax. With the development of spatial light modulators and computing technology, the 3D holograms can now be displayed in real time[11,12]. However, the lack of space bandwidth product of the

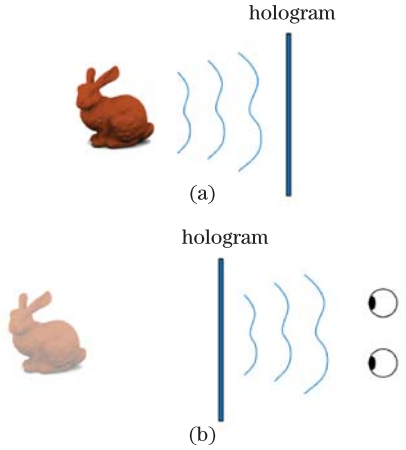

Fig. 1. (Color online) (a) Recording and (b) reconstruction processes of holography.

holographic system limits its optical performances, including the field of view and image size. Though many efforts have been done to expand the bandwidth of the holographic system, such as tiling multiple modulators, developing new types of SLMs, and refreshable emulsion, the holographic display is still far from mass commercialization. Volumetric display uses voxels to present the actual points of the 3D scene in space with the help of spinning diffusive screen, LED array, or passive optical scatters[13,14]. It can provide accurate spatial position for each point and can achieve 360-degree viewing angle. However, the entire display volume is transparent, and this leads it incapable to provide the occlusion effect.

In this review, the discussion is limited into two classes of 3D display technologies: holographic display and light field display, since they have better performances in providing the depth information compared with other methods. These two techniques are descripted in wave and ray optics, respectively. Their display mechanisms are analyzed along with the depth cues of human visual system, and limits imposed on the techniques are also discussed.

2. Holographic display

Holography was invented in 1948 by Dennis Gabor[15] to correct the aberrations of microscopic system, but only became practical for display usage after laser (coherent light source) became commercially available. The off-axis transmission hologram introduced by Leith and Upatniek[16] opened a new horizon of display holography. It can be seen as the foundation of holographic display techniques afterwards. Holography also has a wide range of applications in areas including data storage[17,18], optical metrology[19], microscopy[20], and diffractive optical elements (DOEs) manufacturing[21]. Light field 3D display systems have also been benefited from holographic optical elements (HOEs), which will be discussed in the following section.

Holography can produce depth information of the 3D scene because of its ability to reconstruct the whole optical wavefront, including intensity and direction of a light field. Holography usually takes two steps to operate the wavefront: a recording step, and a reconstruction step. As is shown in Fig. 1(a), the recording step is the process in which the object wavefront emitted by the 3D scene is captured on the hologram plane:

$$O(x,y) = |O(x,y)| \exp\left[j\varphi_O(x,y)\right], \tag{1}$$

where $|O(x,y)|$ is the amplitude distribution and $\varphi_O(x,y)$ is the phase distribution, respectively. The phase distribution is crucial to the reconstruction of the 3D scene, since it determines the direction of the light. Interference pattern is used to encode the phase distribution into the amplitude hologram, which can be attained using both optically and numerically based methods[22]. Alternatively, the phase distribution can be directly recorded in a phase hologram[23]. After storing the wavefront information of the 3D scene, the hologram is ready for optical reconstruction. During reconstruction, the hologram diffracts the illumination beam to the viewer. The viewer could see the 3D scene through this holographic window, as is shown in Fig. 1(b). According to angular spectrum theory in Fourier optics, the optical wavefront on the hologram plane can be decomposed into a sum of plane waves at different angles. These plane waves represent different spatial frequencies of the wavefront, as is shown in Fig. 2. The hologram can be seen as a specialized diffraction grating that diffracts light along multiple angular directions and finally forms the 3D shape of the original scene. The optical performance and the viewing parameters of the holographic display system are hugely affected by the geometric specifications of the hologram. Specifically, the viewing angle is determined by the spatial resolution of the hologram. It can be deduced from the grating equation:

$$\sin\theta = f_{\max}\lambda = \frac{1}{2d}\lambda, \tag{2}$$

where θ is the maximum diffraction angle, $f_{\max}$ is the maximum spatial frequency of the hologram, λ is the wavelength of the diffracted light, and d is the sampling distance of the hologram pixels. We can see that larger diffraction angle can be attained with finer grating scale. Figure 3 illustrates the relationship between viewing angle $\beta = 2\theta$ and the sampling distance of the hologram. The hologram size L is the multiplication of sampling distance (d) and the number of samples (N) in one dimension:

$$L = dN. \tag{3}$$

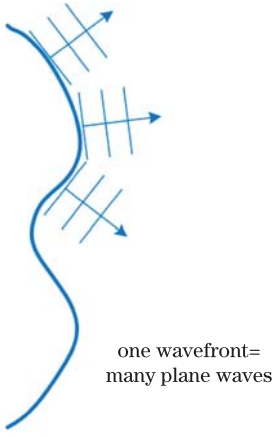

Fig. 2. (Color online) Decomposing an optical wavefront into multiple plane waves using angular spectrum.

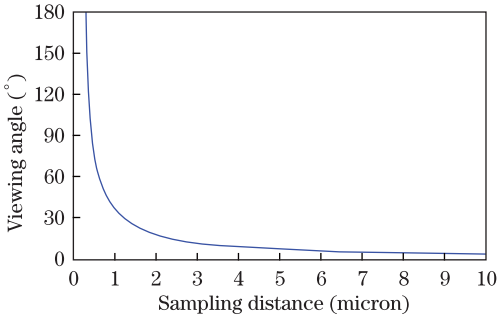

Fig. 3. (Color online) Relationship between viewing angle and sampling distance of a hologram.

We can use additional optical systems to trade off the viewing angle against the hologram size, but the product of viewing angle and hologram size is limited by the following formula:

$$L \sin \beta \propto N. \tag{4}$$

This illustrates that the optical performance of the holographic system is determined by the space-bandwidth product of the hologram. The space-bandwidth product is the product of the linear dimension of the hologram by its maximum spatial frequency, which measures the amount of information that can be produced by the optical system.

Holograms recorded in photosensitive materials can provide enough space-bandwidth product and hence the 3D images is produced with high visual quality. However, the space-bandwidth products of dynamic holographic displays are much lower than the static ones, and it bottlenecks the commercialization of the electronic holographic display system. Hence many works have been done to produce better optical performance through expanding the system space-bandwidth product. The holo-video systems from Media Lab at MIT use acousto-optic modulators combined with the mechanical scanners to produce high bandwidth horizontal-parallax-only (HPO) holograms[24,25]. The group's recent work demonstrated a new integrated-optics platform for holographic video consisting of arrays guided-wave acousto-optic devices. This holographic video architecture can trade off its enormous pixel bandwidth for display extent, viewing angle and the frame rate[26]. Slinger *et al.*[27] at QinetiQ proposed an active tiling system to achieve an extremely high space-bandwidth product. The heart of the system is a set of replication optics that produces multiple images of an electrically addressed spatial light modulator (SLM) to an optically addressed SLM. By stacking 4 electrical-to-optical modules like bricks, the active tiling system can produce more than 100 Mega-pixel data. Recently, many multi-SLM based holographic display systems have been developed. These techniques either tile the SLMs on a plane or on an arc to increase the size and the field of view[28]. Blanche *et al.*[29,30] at University of Arizona collaborated with Nitto Denko developed a system using refreshable photorefractive polymer to record the holograms. This system can be seen as an intermediate technique of holo-video display and holographic stereogram.

Apart from the device, computation is another factor that would affect the image quality of the holographic display system. The computation process determines whether the full potential of the holographic device is activated. Through numerical methods, the holograms can be generated without the real objects and the complicated interference recording system. In order to generate 3D hologram, two steps are usually needed. The first is the mathematical description of the 3D scene, and the second is the algorithm to transfer the 3D scene into light distribution on the hologram plane. The algorithm is directly related to the image quality and the computation speed. Most of the current algorithms for synthesizing the computer generated holograms (CGHs) are physically based methods. These kinds of algorithms simulate the optical transmission process from the 3D objects to a hologram plane[31,32]. The objects are often divided into point sources or planar segments, which can provide precise description for the 3D scene. Hence continuous motion parallax and accurate depth information can be reconstructed during optical reconstruction. However, since the physically based methods focus on the wave propagation simulations, it is often hard for them to integrate with rendering techniques of computer graphics, hence it makes them difficult to provide the view dependent properties of the 3D scenes, such as shading and occlusion. Recently, several researchers have developed some techniques to solve this problem to produce shading and occlusion effects of the 3D scene, but with more computational cost[33,34]. Holographic stereogram based modeling is another class of methods for computing the CGHs. Holographic stereograms angularly multiplex 2D parallax views that are generated digitally or captured optically[10,35]. Computer graphics rendering techniques can be applied in the stereogram computation to add multiple shading effects and eventually make the 3D scene more realistic. Further, the hologram is segmented into multiple holographic elements (hogels), and the occlusion problem can be automatically solved during the rendering processes in different hogels. However, the holographic stereograms are not fully computed holograms. During reconstruction, each hogel projects a set of plane waves in different directions to form the 2D parallax view, which would cause the lack of depth information of the 3D scene. Hence the holographic stereogram is difficult to reconstruct deep 3D scene with accurate accommodation cue. Several works have been done to add depth information in the holographic stereogram based methods, including phase-added stereogram[36], ray sampling plane technique[37], and diffraction specific coherent panoramagram[38]. These methods utilize the z-buffers to reshape the wavefront emitted from each hogel

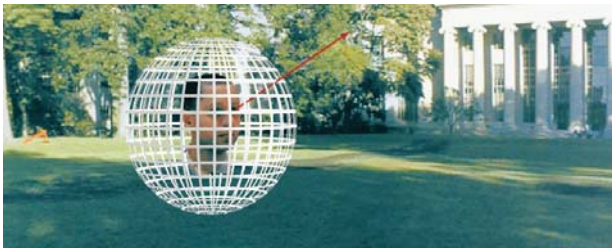

Fig. 4. (Color online) The 5D plenoptic function. (Figure from L. McMillan, "Image-based rendering using image warping," *ACM SIGGRAPH* 1999 courses)

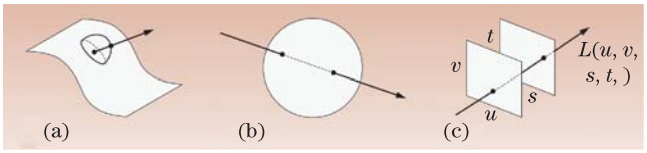

Fig. 5. (Color online) Alternative parameterizations of the 4D light field. (Figure from Ref. [42])

to produce accurate depth information of the 3D scene. For both physically and stereogram based algorithms, computation load is another problem need to be considered in their implements. Due to the parallel property of the CGH generation process, modern graphics processing units (GPUs) that allow general-purpose computing can be used to speed up the computation process[39].

3. Light field display

Light field is a phrase widely used in computer graphics, which is a function that describes the light rays in space. Different with wave optics, it is a concept restricted to geometrical optics and ray is regarded as the fundamental carrier of light. Each ray in free space contains a constant amount of optical energy transmitting along it, and different rays would not interact with each other. Physically, the amount of light traveling along a ray is radiance. It can be denoted by L and measured in watts (W) per steradian (sr) per meter squared $\left(\mathrm{m}^2\right)$. The radiance along all such rays in a region of 3D space illuminated by an unchanging arrangement of lights is called the plenoptic function[40]. The function can be parameterized by coordinates, x, y, and z with angles θ and ϕ. This 5D plenoptic function $L\left(x, y, z, \theta, \phi\right)$ parameterizes every possible ray in the space, hence it can express the image of scene from any viewing position at any viewing angle within the limitations of geometrical optics, as is shown in Fig. 4. The plenoptic function represents light observed from every position in every direction, and it can provide a complete representation of the light rays in a scene, which forms the basis of light field display techniques. While in free space, radiance of light rays does not change along their traveling paths. Hence, the 5D plenoptic function can be expressed as a 4D light field[41,42]. As is shown in Fig. 5, the 4D light field has a variety of representations for parameterizing the light rays. A light ray can be defined by its intersection point with a surface and an additional pair of elevation and azimuth of the ray with respect to the surface normal, as is shown in Fig. 5(a). Also, a pair of points of a sphere can parameterize any light ray passing through it, as is shown in Fig. 5(b). A more commonly used method for describing the light rays is two-plane parameterization, which is shown in Fig. 5(c). Under this situation, a given light ray is defined by its coordinates of intersection with two planes. The light field parameterized in this way is called a light slab. The two-plane parameterization method is widely used for analyzing camera and display architectures.

The light field rendering technique in computer graphics is actually motivated by the holographic stereogram synthesis[43]. Halle's work anticipates the geometry used in Lovey's work[41]. There are some similarities in the full parallax holographic stereogram the integral photography developed by Lippmann in 1908[7]. In integral photography, a lenslet array is placed in close proximity to the photosensitive medium. Each small lens can capture a slightly different perspective image of the 3D scene than its neighbor, and an array of 2D parallax views is recorded in the film through the lenslet. The resulting image viewed through the lens array would create discrete perspectives at corresponding directions. Hence it can enable the viewer to perceive the 3D depth information. Furthermore, a pinhole array can be used instead of the lenslet, which results in a parallax barriers display[44]. However, both integral photography and parallax barriers suffer from low resolution problems due to the trade-off relationship between the spatial and angular sampling numbers, which means the resolution of projected images is reduced with the increase in the number of viewing directions. While in full parallax holographic stereogram, the lens array in integral photography is replaced by a diffractive element performing the same function, and this breaks the geometrical limitation of parallax based techniques (including integral photography and parallax barriers) and can provide finer sampling to the light field in 3D space.

Recently, different with conventional parallax based techniques, some new methods have been developed to produce light field display that can break the trade-off relationship of spatial resolution and number of perspectives the way that parallax barriers and integral photography are forced to do. Jones *et al.*[8] from University of Southern California demonstrated an auto stereoscopic light field display system using a high-speed digital light processing (DLP) projector along with a spinning anisotropic screen. This system can project 360-degree views with 1.25 degree separation horizontally. Different with volumetric displays that use a spinning diffuse screen to scatter light in all directions, they use anisotropic holographic diffuser bonded onto a first surface mirror. The anisotropic diffuser is used to reflect each projector pixel to a narrow range of viewpoints to mimic the light field. Xia *et al.*[45] from Zhejiang University also developed a 360-degree light field display system. Their system used a different architecture that floats the 3D scene above the spinning screen and allows the viewer to touch. Instead of time multiplexing technique, a class of spatial multiplexing techniques have emerged[46,47]. Balogh *et al.*[47] from Holografika Ltd. developed an optical display system to present the 3D light field with multiple projectors and a holographic screen. The holographic screen directs the light beams generated in the optical modules to different directions, and it forms a continuous parallax view. Most of these projector-based light field display systems provide only the horizontal parallax of the 3D scene. Hence the accommodation cue was demonstrated in the horizontal dimension only within a limited depth range. Through the combination of ray optics and computational processing, compressive light field displays have been developed to break the limits set by purely optical analysis. Wetzstein *et al.*[9] developed tomographic techniques for image synthesis on displays composed of stacked films of light-attenuating material. This technique can create a 4D light field with high resolution and the accommodation is preserved. The same underlying technique is later applied to stacks LCDs for displaying dynamic content[48]. For such compressive light field displays, which require

taking a target 4D light field as an input and solving an optimization problem for image synthesis, usually need massive computations.

To improve the image qualities and the depth properties of current light field display techniques, the gap between reconstructed light field and the target light field of the 3D scene should be narrowed. The increase of space-bandwidth product of the display system would improve the spatial and angular resolutions, and eventually lead to better approximation to the target light field.

4. Discussion and conclusion

Though the light is treated differently in wave optics and ray optics, redistributing the light in 3D space eventually provides us the depth information in both methods. Static full parallax holographic stereogram can be considered as a combination of the holographic and light field technique, which leads to marvelous 3D effects during reconstruction. Recently, several researchers have tried to build a bridge between wave and ray optics through phase space analysis, and used it to analysis the 3D display systems. Zhang *et al.*[49] introduced the connection between wigner distribution function and the light field. Wigner distribution function can be thought as a more rigorous ray-model representation of light that incorporates wave optics phenomena. The function can describe spatial position and spatial frequency of the light simultaneously. Inspired by the wigner distribution function, Oh *et al.*[50] developed a technique based on the augmented light field to model the wave optics effects. The phase space analysis may lead to additional insights and productive applications in 3D displays related to wave and ray optics.

The development of 3D display would rely on joint advances on several different areas, including computer graphics, wave and ray optics, materials, mathematical modeling, and the industry world. The 3D display techniques need extra data to provide the information from the third dimensionality. Hence the space-bandwidth product is an important factor to improve the qualities of the 3D images, both in holographic and light field display architectures. Also, the deeper understanding of the human visual system will play a key role as well.

This work was supported by the National Basic Research Program of China (No. 2013CB328801) and the National Natural Science Foundation of China (No. 61205013).

References

1. C. Wheatstone, Phil. Trans. R. Soc. Lond. **128,** 371 (1838).
2. N. J. Wade, *Brewster and Wheatstone on Vision* (Academic Press, London and New York, 1983).
3. H. Jorke and M. Fritz, in *Proceedings of Electronic Displays* (2003).
4. E. Dubois, in *Proceedings of IEEE International Conference on Acoustics Speech Signal Processing* **3,** 1661 (2001).
5. P. Bos, in *Proceedings of ITEC'91 Annual Conference, Three-Dimensional Image Technology* 603 (1991).
6. F. E. Ives, "Parallax stereogram and process of making same," United States Patent US725567 (1903).
7. G. Lippmann, J. Phys. **7,** 821 (1908).
8. A. Jones, I. McDowall, H. Yamada, M. Bolas, and P. Debevec, ACM Transactions on Graphics (TOG) **26,** 40 (2007).
9. G. Wetzstein, D. Lanman, W. Heidrich, and R. Raskar, ACM Transactions on Graphics (TOG) **30,** 95 (2011).
10. S. A. Benton and V. M. Bove, *Holographic Imaging* (Wiley, Hoboken, 2007).
11. A. Shiraki, N. Takada, M. Niwa, Y. Ichihashi, T. Shimobaba, N. Masuda, and T. Ito, Opt. Express **17,** 16038 (2009).
12. P. Yeh and C. Gu, Chin. Opt. Lett. **11,** 010901 (2013).
13. R. D. Willams and F. Garcia, Jr., Inf. Disp. **4,** 8 (1989).
14. J. Y. Son and S. A. Shestak, Proc. SPIE **4660,** 171 (2002).
15. D. Gabor, Nature **161,** 777 (1948).
16. E. N. Leith and J. Upatnieks, J. Opt. Soc. Amer. **54,** 1295 (1964).
17. S. Luo, K. Chen, L. Cao, G. Liu, Q. He, G. Jin, D. Zeng, and Y. Chen, Opt. Express **13,** 3123 (2005).
18. P. Zijlstra, J. Chon, and M. Gu, Nature **459,** 410 (2009).
19. C. Wagner, S. Seebacher, W. Osten, and W. Jüptner, Appl. Opt. **38,** 4812 (1999).
20. T. Zhang and I. Yamaguchi, Opt. Lett. **23,** 1221 (1998).
21. N. Lai, W. Liang, J. Lin, C. Hsu, and C. Lin, Opt. Express **13,** 9605 (2005).
22 B. R. Brown and A. W. Lohmann, IBM J. Res. Develop. **13,** 160 (1969).
23 L. B. Lesem, P. M. Hirsch, and J. A. Jordan, IBM J. Res. Develop. **13,** 150 (1969).
24 P. St.-Hilaire, S. A. Benton, M. Lucente, M. L. Jepsen, J. Kollin, and H. Yoshikawa, Proc. SPIE **1212,** 174 (1990).
25 D. Smalley, Q. Smithwick, and V. M. Bove, Jr., Proc. SPIE **6488,** 64880L (2007).
26 D. Smalley, Q. Smithwick, V. Bove, J. Barabas, and S. Jolly, Nature **498,** 313 (2013).
27 C. Slinger, C. Cameron, and M. Stanley, IEEE Computer **38,** 46 (2005).
28 F. Yaras, H. Kang, and L. Onural, J. Display Technol. **6,** 443 (2010).
29 S. Tay, P. A. Blanche, R. Voorakaranam, A. V. Tunc, W. Lin, S. Rokutanda, T. Gu, D. Flores, P. Wang, G. Li, P. St.-Hilaire, J. Thomas, R. A. Norwood, M. Yamamoto, and N. Peyghambarian, Nature **451,** 694 (2008).
30 P.-A. Blanche, A. Bablumian, R. Voorakaranam, C. Christenson, W. Lin, T. Gu, D. Flores, P. Wang, W.-Y. Hsieh, M. Kathaperumal, B. Rachwal, O. Siddiqui, J. Thomas, R. A. Norwood, M. Yamamoto, and N. Peyghambarian, Nature **468,** 80 (2010).
31 Y. Ichihashi, H. Nakayama, T. Ito, N. Masuda, T. Shimobaba, A. Shiraki, and T. Sugie, Opt. Express **17,** 13895 (2009).
32 K. Matsushima, Appl. Opt.**44,** 4607 (2005).
33 T. Kurihara and Y. Takaki, Opt. Express **20,** 3529 (2012).
34 H. Zhang, N. Collings, J. Chen, B. Crossland, D. Chu, and J. Xie, Opt. Eng. **50,** 074003 (2011).
35 J. T. McCrickerd and N. George, Appl. Phys. Lett. **12,** 10 (1968).
36 H. Kang, T. Yamaguchi, H. Yoshikawa, S. Kim, and E. Kim, Appl. Opt. **47,** 5784 (2008).
37 K. Wakunami and M. Yamaguchi, Opt. Express **19,** 9086 (2011).
38 Q. Y. J. Smithwick, J. Barabas, D. E. Smalley, and V. M. Bove, Jr., Proc. SPIE **7619,** 761903 (2010).

39 H. Kang, F. Yaras, and L. Onural, Appl. Opt. **48,** H137 (2009).

40 E. H. Adelson and J. R. Bergen, in *Computational Models of Visual Processing*, (MIT Press, Cambridge, 1991) pp. 3-20.

41 M. Levoy and P. Hanrahan, in *Proceedings of the 23rd annual Conference on Computer Graphics and Interactive Techniques* 31 (1996).

42 M. Levoy, Computer **39,** 46 (2006).

43 M. W. Halle, Proc. SPIE **2176,** 73 (1994).

44 H. E. Ives, J. Opt. Soc. Am. **17,** 435 (1928).

45 X. Xia, X. Liu, H. Li, Z. Zheng, H. Wang, Y. Peng, and W. Shen, Opt. Express **21,** 11237 (2013).

46 C. N. Moller and A. R. L. Travis, IEEE Trans. Visual. Comput. Graph. **11,** 228 (2005).

47 T. Balogh and P. T. Kovács, Proc. SPIE **7724,** 772406 (2010)

48 D. Lanman, G. Wetzstein, M. Hirsch, W. Heidrich, and R. Raskar, ACM Transactions on Graphics (TOG) **30,** 186 (2011).

49 Z. Zhang and M. Levoy, in *Proceedings of 2009 IEEE International Conference on Computational Photography* (ICCP) 1 (2009).

50 S. B. Oh, S. Kashyap, R. Garg, S. Chandran, and R. Raskar, Comput. Graph. Forum **29,** 507 (2010).